Angelica dahurica promoted angiogenesis and accelerated diabetic wound healing by regulating pericyte-endotheliocyte exosomes crosstalk through Wnt4/β-catenin signal pathway

Junfen Liu
Chu Hsien-I Memorial Hospital, Tianjin Medical University
Wangna Tang
Chu Hsien-I Memorial Hospital, Tianjin Medical University
Cailing Gao
Chu Hsien-I Memorial Hospital, Tianjin Medical University
Wenjie Liu
Chu Hsien-I Memorial Hospital, Tianjin Medical University
Linlin Wang
The First Affiliated Hospital of Hebei North University
Congqing Pan (cq.pan@163.com)
Chu Hsien-I Memorial Hospital, Tianjin Medical University

Article

Keywords:

Posted Date: March 28th, 2023

DOI: https://doi.org/10.21203/rs.3.rs-2700421/v1

Additional Declarations: No competing interests reported.

Angelica dahurica promoted angiogenesis and accelerated diabetic wound healing by regulating pericyte-endotheliocyte exosomes crosstalk through Wnt4/β-catenin signal pathway

Junfen Liu[1,2†], Wangna Tang[1†], Cailing Gao[1†], Wenjie Liu[1], Linlin Wang[2], Congqing Pan[1]*

[1]NHC Key Laboratory of Hormones and Development, Tianjin Key Laboratory of Metabolic Diseases, Chu Hsien-I Memorial Hospital & Tianjin Institute of Endocrinology, Tianjin Medical University, Tianjin, 300134, People's Republic of China

[2]The First Affiliated Hospital of Hebei North University, Hebei, 075000, People's Republic of China

***Correspondence:**

Congqing Pan: NHC Key Laboratory of Hormones and Development, Tianjin Key Laboratory of Metabolic Diseases, Chu Hsien-I Memorial Hospital & Tianjin Institute of Endocrinology, Tianjin Medical University, Tianjin, China. Email: cq.pan@163.com

† These authors have contributed equally to this work and share the first authorship.

Abstract

Diabetic foot ulcers (DFUs) are a multifactorial complication of diabetes mellitus associated with impaired angiogenesis. Potentially effective treatments for such wounds are currently unknown. Cross-talk between pericyte and endothelial cell

exosomes has been reported as a therapeutic strategy for treating DFUs. By regulating pericyte-endotheliocyte exosomes crosstalk, Angelica dahurica (AD) promoted angiogenesis and accelerated diabetic wound healing in this study. AD stimulated the migration and angiogenic tubule formation of human umbilical vein endothelial cells (HUVECs) by stimulating exosomes derived from human cerebrovascular pericytes (HBVPs), which was accompanied by increased protein expressions of Wnt4, β-catenin, and cyclinD1. In addition, the Wnt/β-catenin pathway inhibitor XAV939 reversed the activation of the Wnt4/β-catenin signalling pathway in HUVECs by AD. In the STZ-induced cutaneous wound rat model, AD enhanced angiogenesis and collagen deposition in vivo, resulting in a faster wound healing rate and a smaller wound area. AD concurrently promoted capillary formation by activating the Wnt4/β-catenin signalling pathway. AD promoted angiogenesis of HUVECs in vitro by regulating HBVPs-derived exosomes via the Wnt4/β-catenin signal pathway, thereby enhancing vascularization in regenerated tissue and promoting wound healing in vivo. The research indicated that AD could be used as a treatment for enhancing angiogenesis in diabetic wound healing.

Introduction

Diabetes is a chronic metabolic disease with numerous complications. Chronic foot ulcerations are common in diabetic patients[1]. Pathogenesis of diabetic foot ulcers (DFUs) is linked to vascular damage and abnormal neural system changes [2]. Globally, it is estimated that 15-25% of diabetic patients will suffer from DFUs in their lifetime [3], with some even requiring amputation of the lower extremities, which negatively impacts patient quality of life and places a significant burden on medical institutions [4,5].

However, the current treatments for DFUs, including anti-infection methods, debridement, lesion location management of peripheral vessels, and wound dressing, are not satisfactory [6,7]. In the future, more research will be necessary to develop effective treatments for DFUs and their underlying mechanisms.

Wound healing is a complex process linked to angiogenesis, which promotes vessel growth, proliferation, and maturation [8-10]. Exosomes mediate cell-to-cell crosstalk through the transfer of intracellular components including DNA, RNA, and proteins [11] and promote cutaneous wound healing by promoting collagen synthesis and angiogenesis. Zhang et al. reported that exosomes extracted from adipose stem cells in vitro promoted the tube formation of HUVECs in a high glucose environment [12], suggesting that exosomes enhance the angiogenesis process and wound closure rate in diabetes mellitus. According to a study, pericytes are specialised cells located abluminally of endothelial cells [13], Furthermore, direct contact and paracrine regulation between pericytes and endothelial cells are essential for angiogenesis [14]. However, the diabetic disease state can significantly affect the crosstalk or function of exosomes between pericytes and endothelial cells, thereby delaying wound healing in diabetes [15]. Therefore, the crosstalk of exosomes between pericytes and endothelial cells under conditions of high glucose is essential for vascular maturation. In spite of this, the mechanisms and signal molecules of pericyte-endotheliocyte crosstalk in diabetic conditions remain obscure.

Wnt family glycolipoproteins regulate embryonic development, homeostasis, cell proliferation, and differentiation [16,17]. Wnt/β-catenin pathway, the canonical Wnt pathway, is essential for wound healing, wound angiogenesis, and epithelial remodelling [18]. According to the literature, the expression of vascular endothelial cells is influenced by Wnt/β-catenin pathway relative effectors when exposed to high glucose for an extended period of time [19]. In addition, another study [20] demonstrates that the downregulation of the Wnt/β-catenin pathway is associated with diabetes. Wnt4 is a member of the Wnt family and is known to be transferred by exosomes to play a role in angiogenesis. For example, exosomes derived from human umbilical cord mesenchymal stem cells have been shown to promote angiogenesis by delivering Wnt4 to activate Wnt/β-catenin in endothelial cells [21]. Based on these findings, we hypothesise that Wnt4 was abundant in cell-derived exosomes and mediated the functions of endothelial cells to promote angiogenesis.

Herbal medicines are still used to develop new drugs and treat diseases. Angelica dahurica (AD) is a traditional Chinese herbal remedy known as Bai-zhi in Chinese. It contains numerous biologically active compounds, including furanocoumarins, imperatorin, isoimperatorin, oxypeucedanin hydrate, and others [22]. Numerous studies indicate that AD plays a role in the treatment of pain, cold fever, furunculosis, and certain skin diseases [23,24]. Our previous research demonstrated that AD can increase the formation of new blood vessels and promote wound healing in diabetic mice [25,26]. In addition, the communication between pericytes and endothelial cells plays a role in diabetic

wound healing. However, the effects of AD on the crosstalk between pericytes and endothelial cells during wound healing in diabetics remain unknown. We hypothesise that AD may promote diabetic wound healing by regulating pericyte-endothelial cell communication.

The human umbilical vein endothelial cells (HUVECs) and human cerebrovascular pericytes (HBVPs) were utilised in this study to determine the angiogenesis-promoting effect and underlying mechanism of AD. A diabetic full-thickness cutaneous wound model was also used to assess the AD's curative capacity. Given that the crosstalk of exosomes between pericytes and endothelial cells is essential for vascular development and maturation, we hypothesise that AD may facilitate diabetic wound healing by regulating pericyte-endotheliocyte exosomes crosstalk via the Wnt4/β-catenin signal pathway. In vivo and in vitro experiments were conducted to determine the effects of AD and confirm the regulatory pathogenesis that AD accelerates diabetes-related wound healing by regulating pericyte-endotheliocyte exosomes crosstalk via the Wnt4/β-catenin signal pathway. This study aims to develop a novel therapeutic approach for the treatment of DFUs.

Results

AD promotes wound healing in STZ rats. On rats, full-thickness cutaneous wounds were created and observed on days 0, 3, 7, and 11 following surgery. As shown in **Figure 1A**, diabetic wounds healed more slowly in STZ rats than in CON rats. In contrast, wound area images decreased when treated with AD, and the wound area of STZ+AD

rats on day 11 after surgery was significantly narrower than that of STZ rats (**Figure 1A**). In the STZ group, the rate of healing was considerably slower than in the CON group. However, the STZ+AD group had a faster wound healing rate than the STZ group (**Figure 1B**). ALT (**FigureS1 C**), AST (**FigureS1 D**), BUN (**FigureS1 E**), and Scr (**FigureS1 F**) did not differ significantly between the three groups. And the administration of AD had no effect on blood glucose levels (**Figure S1 A**) or body mass (**FigureS1 B**).

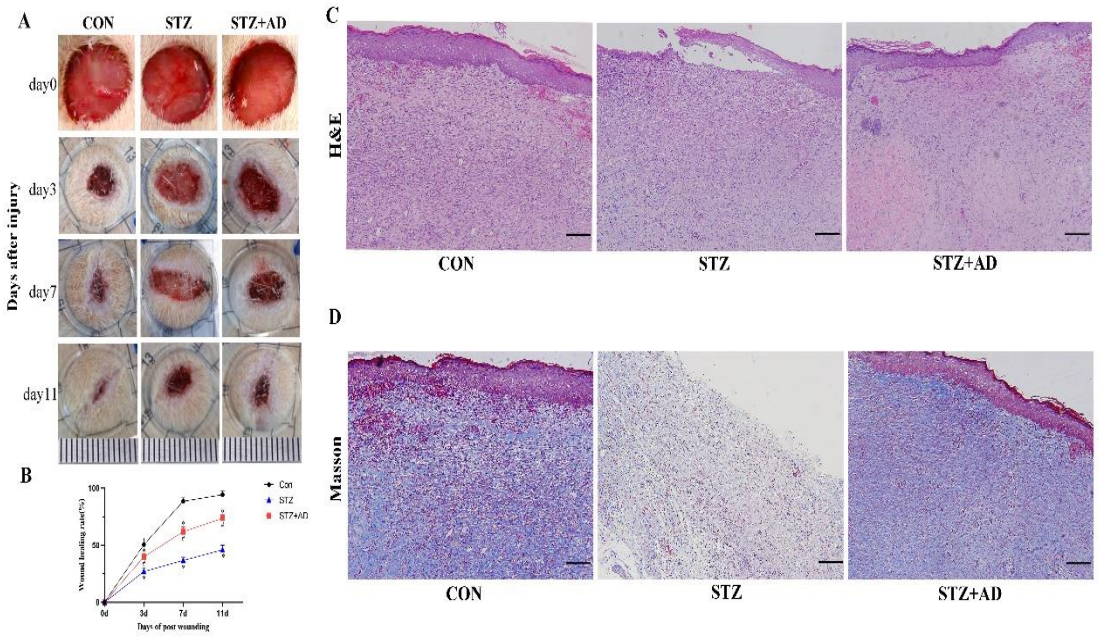

Figure 1. AD promotes wound healing and structural improvement in STZ rats.

AD increases the angiogenesis and collagen deposition in vivo. The skin tissues of STZ rats were stained with H&E to measure the histopathologic changes. As depicted in **Figure 1C**, H&E staining revealed that STZ rats had fewer blood vessels and slower wound healing compared to the CON group. On day 11, H&E staining revealed advanced wound closure and thicker granulation tissue in STZ+AD rats compared to STZ

rats. Masson trichrome staining was used to evaluate collagen deposition and skin wound maturation. Masson trichrome staining revealed substantial deposition of collagen in the AD intervention group (**Figure 1D**). Immunohistochemistry results on day 11 indicated that the expression of Wnt4 was greater in the STZ+AD group than in the STZ group (**Figure 2A, B**). In order to confirm the effects of the Wnt4/β-catenin pathway in diabetic wound rats, β-catenin immunofluorescence was performed on wound tissue. STZ+AD rats exhibited higher fluorescence intensity of skin wound tissues, similar to CON rats, compared to STZ rats (**Figure 2C**). CD31 and CD146 are endothelial cell and pericyte cell markers, respectively. In the CON group, levels of CD31 and CD146 were high. Additionally, the double staining of CD31+CD146 revealed that STZ+AD rats had a greater number of newly formed and mature blood vessels than STZ rats (**Figure 2D, E**).

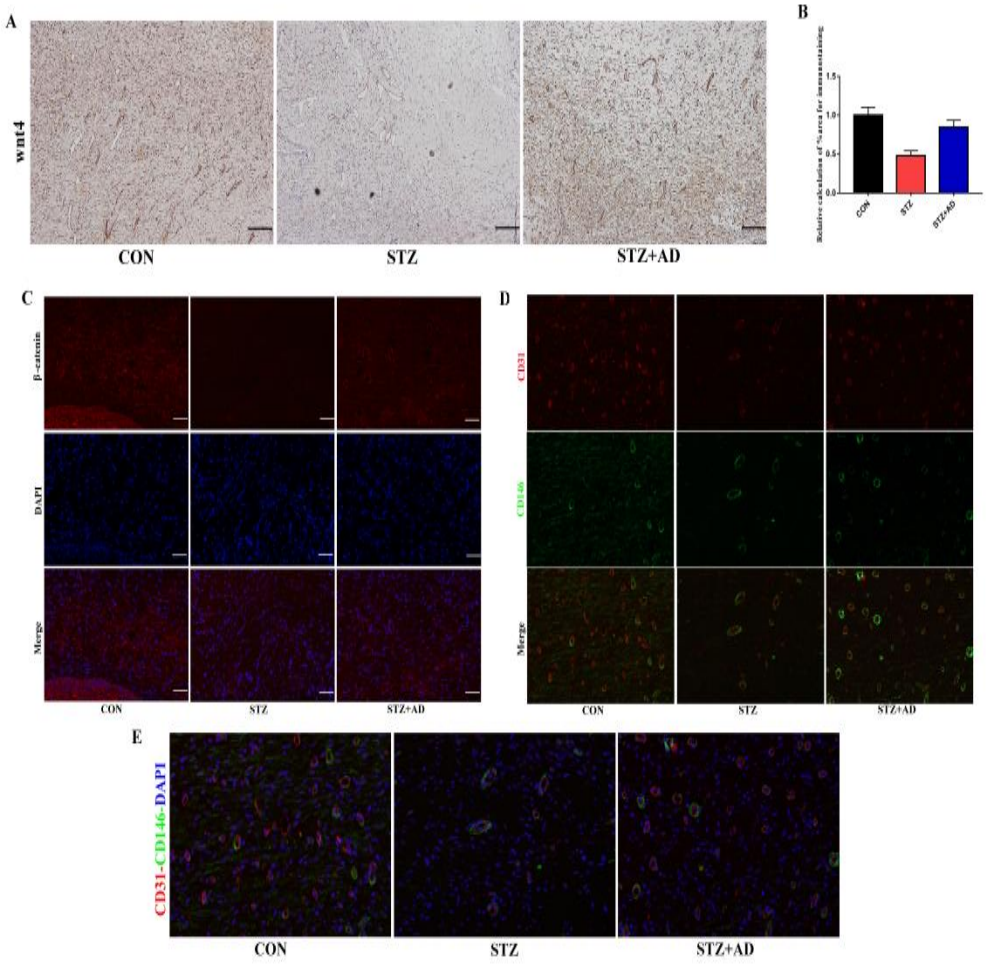

Figure 2. AD increases the angiogenesis in STZ rats.

AD boosts angiogenesis through Wnt4/β-catenin pathway in vivo. The Wnt4/β-catenin pathway has been implicated in angiogenesis. Therefore, we examined the relative proteins of the Wnt4/β-catenin axis following in vivo AD treatment. Western blotting (**Figures 3A, B**) revealed that the levels of Wnt4, β-catenin, and cyclinD1 were significantly higher in the skin wound tissues of rats in the STZ+AD group than in the STZ group. In addition, the western blot results mirrored the immunofluorescence (**Figure 2C**) and immunohistochemistry (**Figures 2A, B**) results of wound tissues.

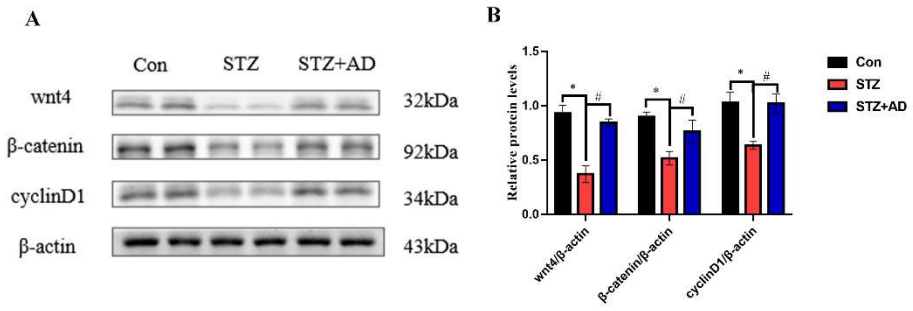

Figure 3. AD boosts angiogenesis through Wnt4/β-catenin pathway in vivo.

The characterization of exosome derived from HBVPs. Western blot, transmission electron microscopy, and NTA were used to identify the exosomes derived from HBVPs under various conditions. In addition, BCA was used to measure the concentrations of exosomes derived from HBVPs (**Figure 4D**). Protein markers of exosomes demonstrated that ALIX, Hsc70, and TSG101 were highly expressed in all groups, whereas Calnexin was not detected in any of the groups (**Figure 4C**). Transmission electron microscopy was used to evaluate the exosome morphologies derived from HBVPs (**Figure 4E**). Exosome sizes were centred on approximately 100 nm (**Figure 4F**).

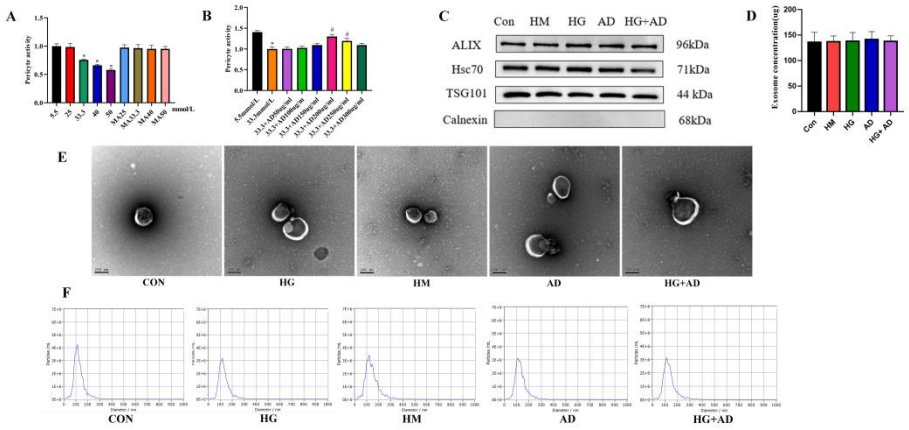

Figure 4. The characterization of exosome derived from HBVPs.

Exosome ingestion and the effects of exosome derived from HBVPs on HUVEC vitality. Exosomes (in red) derived from HBVPs with different interventions can be ingested by HUVEC after 24 hours of incubation, as shown in **Figure 5A**. To further elucidate the effects of exosomes derived from HBVPs on endothelial cell vitality, HUVECs were maintained for 24 hours with different concentrations of exosomes derived from different sources (0.01-40 μg/mL, **Figure 5B**). Exosomes derived from CON group HBVPs and HM group HBVPs at concentrations of 10 μg/mL (Figure 5B-a, c) are effective in treating HUVECs. Exosomes derived from AD group or HG+AD group HBVPs at 20 μg/mL (**Figure 5B-d, e**) are effective in treating HUVECs. When the concentration of exosomes derived from HG group HBVPs was greater than 5 μg/mL, the viability of HUVECs was compromised (**Figure 5B-b**). Considering that 10 μg/mL of exosomes derived from HBVPs with various interventions had the least effect on the activity of HUVECs, this concentration was selected for further study.

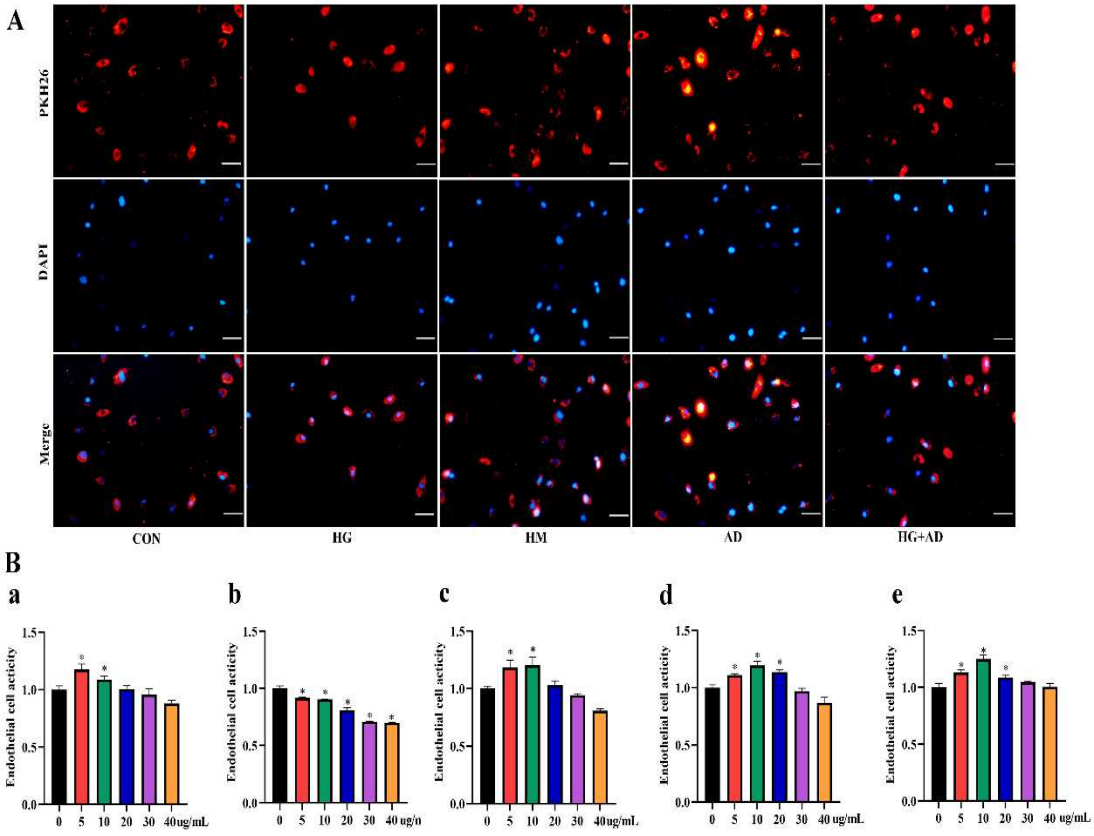

Figure 5. Exosome ingestion and the effects of exosome derived from HBVPs on HUVECs vitality.

AD promotes the migration and angiogenic tubule formation of HUVECs by regulating exosomes derived from HBVPs. Scratch assay and tube formation assay were conducted to examine the effects of HBVPs-derived exosomes on HUVECs functions. Exosomes extracted from HBVPs maintained in high glucose (HG-Exo group) decreased the migration rate of HUVECs relative to the CON-Exo group (**Figure 6A, B**). Similarly, we designed the mannitol (HM-Exo) group to exclude the influence of cell osmolality, and there were no significant differences in migration rates between the HM-Exo and CON-Exo groups (**Figures 6A, B**). As shown in **Figures 6C and D**, the exosomes extracted from the HG+AD-Exo group increased the migration rate of

HUVECs compared to the HG-Exo group. Moreover, consistent with the scratch assay, tube formation assay showed the parallel results. HG-Exo group had fewer lymph nodes and shorter tubes than CON-Exo group, but these outcomes were reversed by AD intervention (**Figures 6E-J**).

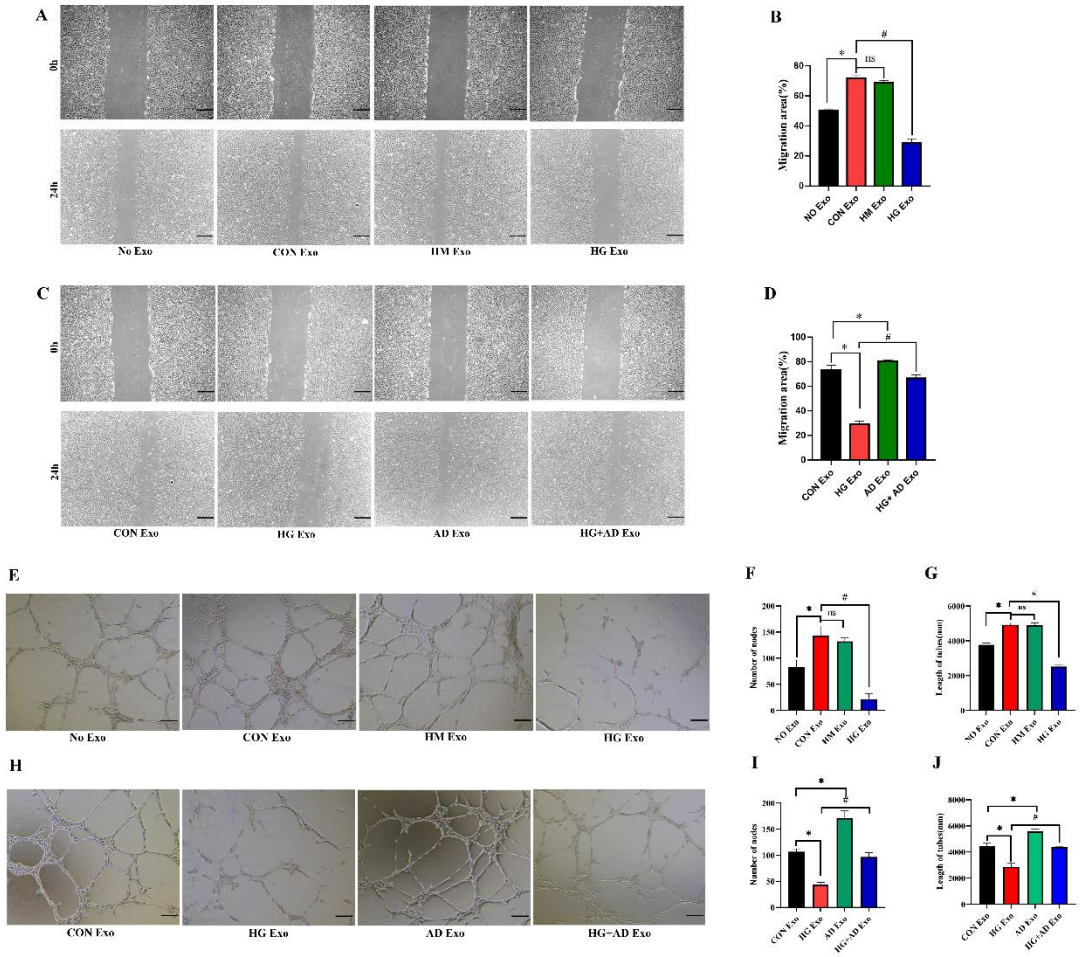

Figure 6. AD promotes the migration and angiogenic tubule formation of HUVECs by regulating exosomes derived from HBVPs.

AD improves the angiogenesis by regulating pericyte-endotheliocyte exosomes crosstalk through Wnt4/β-catenin signal pathway. The Wnt4/β-catenin pathway was essential for angiogenesis. We measured relative protein concentrations in vitro.

Western blotting revealed that the levels of Wnt4, β-catenin, and cyclinD1 were lower in the HG-Exo group compared to the CON-Exo group (**Figures 7A-D**). In contrast, these proteins were elevated in the HG+AD-Exo group (**Figures 7A-D**). To verify the effects of AD on the Wnt4/β-catenin pathway, an inhibitor of the Wnt/β-catenin signalling pathway, XAV939, was utilised in vitro. The western blot (**Figures 7E-H**) revealed that XAV939 inhibited the levels of Wnt4, β-catenin, and cyclinD1. Moreover, AD cannot reverse the effects of inhibition.

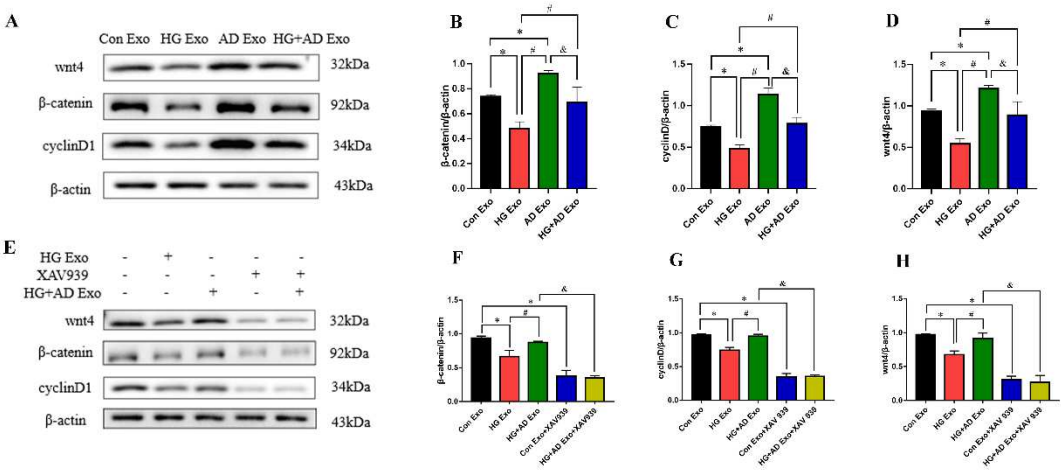

Figure 7. AD improves the angiogenesis by regulating pericyte-endotheliocyte exosomes crosstalk through Wnt4/β-catenin signal pathway.

Discussion

Angiogenesis disorders in diabetic wounds slowed the healing of diabetic foot ulcers (DFUs). Current research has uncovered a novel AD mechanism that accelerates diabetic wound healing by enhancing intercellular communication via exosomes. This study demonstrates that exosomes derived from HBVPs can promote the migration and angiogenic tubule formation of HUVECs via the Wnt4/β-catenin signal pathway to

accelerate angiogenesis and diabetic wound healing. This study highlights the AD regulated pericyte-endotheliocyte exosomes crosstalk. The possible mechanism is that AD-stimulated exosomes upregulate the expression of Wnt4, β-catenin, and cyclinD1 in HUVECs.

Exosomes play a crucial role in diabetic wound healing, promoting intercellular communication to speed up angiogenesis and collagen synthesis [12]. When cells are exposed to a high-glucose environment, a decline in pericyte number, dysfunctional pericytes, and endothelial cell dysfunction have been observed, according to studies [27,28]. In contrast, endothelial cells played a positive role in angiogenesis via exosomes produced by other cells [12]. Exosomes extracted from human amniotic epithelial cells were found to increase capillary density in diabetic mouse models in a study by Wei et al [29]. Exosomes extracted from mesenchymal stem cells and pioglitazone were found to increase the angiogenesis capability of HUVECs, according to a previous study [30]. These studies indicate that exosomes derived from various cell types have the potential to enhance endothelial cells' ability to promote angiogenesis in diabetic environments. In diabetic wound healing, the pericyte-endotheliocyte exosomes crosstalk is unclear. As a result, we investigated intercellular communication with exosomes in a diabetic environment. Consistent with the size of exosomes reported in previous studies [31-33], the sizes of exosomes derived from HBVPs were centred around 100 nm, and HUVECs can consume HBVPs-extracted exosomes. In addition, we discovered that HBVPs-derived exosomes in high glucose conditions impaired the migration rate and tubule formation ability of

HUVECs. In addition, in the STZ rat models, fewer blood vessels, delayed wound closure, and decreased collagen deposition were observed compared to CON rats. On the basis of these findings, we hypothesised that exosomes extracted from HBVPs in different culture conditions could influence the angiogenesis capacity of HUVECs. Therefore, we attempt to discover a novel drug that promotes angiogenesis in diabetic wound healing.

Angelica Dahurica (AD) is a common treatment for furunculosis and other skin diseases in China. It is a traditional Chinese medicine. Numerous studies suggest that AD regulates angiogenesis during diabetic wound healing. According to a previous study [33], AD promoted diabetic wound healing by enhancing the function of endothelial cells. Moreover, AD treatment demonstrated a clear capacity to expedite wound healing in infected wounds [34]. Moreover, direct contact and paracrine regulation between pericytes and endothelial cells are essential for angiogenesis [14]. Despite this, the effects of AD treatment on the communication between pericytes and endothelial cells remain unclear. In this study, in vivo and in vitro experiments were conducted to determine the effects of AD and to confirm the regulatory pathogenesis that AD accelerates diabetes-related wound healing by regulating pericyte-endotheliocyte exosomes crosstalk. Compared to the HG-Exo group, the exosomes extracted from the HG+AD-Exo group increased the rate of migration, the number of nodes, and the length of tubes in HUVECs. In addition, on day 11 after surgery, the wound area of STZ+AD rats was significantly smaller than that of STZ rats. In STZ+AD rats, H&E staining revealed more advanced wound

closure and denser granulation tissue than in STZ rats. In AD intervention rats, Masson trichrome staining revealed significant collagen deposition. By regulating pericyte-endotheliocyte exosomes crosstalk, our results suggest that AD may improve wound healing in a full-thickness cutaneous wound healing model in STZ rats.

The Wnt/β-catenin pathway is essential for wound healing, wound angiogenesis, and epithelial remodelling [18,35,36]. Wnt4 is known to be transferred by exosomes to participate in angiogenesis [21]. Wnt4 is a member of the Wnt family. According to a previous study, exosomes derived from mesenchymal stem cells can deliver Wnt4 to promote angiogenesis in cutaneous wound healing [37]. β-catenin is an essential regulator of cell adhesion and a key component of the Wnt pathway [38]. Previous research indicated that when the levels of Wnt and β-catenin were increased, epidermal cell proliferation and migration were enhanced, and the rate of wound healing was accelerated [39,40]. Similar to previous research, our findings indicated that the relative protein expressions of Wnt4, β-catenin, and cyclinD1 were significantly reduced in the skin wound tissues of STZ group rats, whereas the protein levels were increased in AD-treated rats compared to STZ group rats. With western blot, β-catenin immunofluorescence and Wnt4 immunohistochemistry yielded identical results. Based on these findings, we demonstrated that AD increased in vivo angiogenesis via the Wnt4/β-catenin pathway. Additionally, we performed double immunofluorescence staining for CD31 and CD146. Our research demonstrated that the CON group was rich in CD31 and CD146. AD treatment reversed the decrease in CD31+CD146 observed in STZ-treated rats. Considering CD31 and

CD146 are endothelial cell and pericyte cell markers, respectively [41]. We hypothesised that AD could regulate endothelial cells and pericytes to promote wound healing in diabetics. In the current study, Western blotting revealed that the levels of Wnt4, β-catenin, and cyclinD1 were lower in the HG-Exo group. In contrast, these proteins were elevated in the HG+AD-Exo group. To verify the effects of AD on the Wnt4/β-catenin pathway, the Wnt/β-catenin pathway inhibitor was utilised in vitro. The Western blot results indicated that AD cannot reverse the inhibited protein levels of Wnt4, β-catenin, and cyclinD1. In a full-thickness cutaneous wound healing model in STZ rats, we hypothesised that AD therapy improved angiogenesis by regulating pericyte-endotheliocyte exosomes crosstalk via the Wnt4/β-catenin signal pathway. However, our study focuses primarily on the pericyte-endotheliocyte exosomes crosstalk response associated with diabetic wound healing, highlighting the need for additional research on the other important cells and intracellular components associated with diabetic wound healing.

Conclusion

This study demonstrated that AD stimulated the angiogenesis of HUVECs in vitro by regulating HBVPs-derived exosomes via the Wnt4/β-catenin signal pathway, thereby increasing vascularization in regenerated tissue and facilitating wound healing in vivo. Therefore, the preliminary conclusion is that AD therapy improved angiogenesis by regulating pericyte-endotheliocyte exosomes crosstalk via the Wnt4/β-catenin signal pathway in a full-thickness cutaneous wound healing model, thereby providing

a novel mechanism and method for AD in the treatment of diabetic wound healing.

Materials and Methods

Diabetic rat skin wound model and treatment. All experimental procedures were complied with guidelines of the Guide for the Care and Use of Laboratory Animals of the National Institutes of Health. The study was conducted with Institutional approval from Tianjin Medical University Animal Welfare and Ethical Review Board and in accordance with the ARRIVE guidelines. Seven-week-old Sprague-Dawley (SD) rats (male, 334.5±14.2 g) were purchased from SPF Biotechnology Co. Ltd. (Beijing, China). All rats were conducted a one-week acclimatization period and housed in polycarbonate cages with a 12:12h light/dark cycle at 22-25°C, stable humidity with ad libitum access to standard diet.

The SD rats were randomly divided into control group (N = 10) or diabetic group (N = 20). To generate the diabetic rat model, streptozotocin (STZ, 45 mg/kg, Sigma, USA) (dissolved in 0.1 M citrate buffer, pH 4.5) was injected to diabetic group rats by tail vein fasted for 12 h. The control rats treated with the same volume citrate buffer. The tail blood glucose levels above 16.7 mmol/L for 3 days were diagnosed with diabetes. 2 rats were eliminated from diabetic group for the blood glucose below 16.7 mmol/L. After 10 control group rats and 18 diabetic rats were anesthetized with chloralhydrate, the dorsal skin was shaved and sterilized with 75% ethyl alcohol, two circular sterile wounds on the back of the rats were created by 15-mm punch biopsy tool. After the skin wound models were completed, 18 diabetic rats were randomly divided into STZ group (N = 9) and STZ+AD group (N = 9), the control group (N = 10) which

served as the normal control group (Con group). The Con group and STZ group received the same dose vehicle, rats in the STZ+AD group intragastrically received Angelica dahurica (Yi fang Pharmaceutical. INC Guangdong. China) at a dose of 12.5 g/kg/d by oral gavage. All rats accepted the 11 days treatment period. And the postoperative rats were housed individually.

The body weight and blood glucose from tail vein blood of rats were calculated at days 0, 7 (day 0 after surgery) and 18 (day 11 after surgery) after STZ injected. After the intervention, all animals received an intraperitoneal injection of sodium pentobarbital, then anesthetized, collected the blood samples and sacrificed, lastly, the wounds were removed using scissors and rapidly collected for further experiments.

Analysis of Wound Closure Rate. The conditions of wound closure were observed by photographs obtained on days 0, 3, 7 and 11 after surgery and analyzed by Image-Pro Plus 6.0 software (NIH, USA). The wound healing rate was calculated using the following equation: wound healing rate (%) = (W0 − Wt)/W0 × 100, where W0 is the aera of wound after surgery, and Wt is the wound area at days 0, 3, 7 and 11 after surgery.

Blood measurements. The levels of serum creatinine (Scr), blood urea nitrogen (BUN), alanine aminotransferase (ALT) and aspartate aminotransferase (AST) were measured by standard automatic laboratory analysers (Roche, Switzerland) at days 0 and 11 after surgery.

Histology, immunohistochemical and immunofluorescent staining. After wound

tissues and the surrounding healthy skin of rats were collected, the skin tissues were immersed by 4% paraformaldehyde, embedded into paraffin, and cut it into 4μm continuous slices. The optical microscope (Olympus CKX41, Tokyo, Japan) was used to observe the tissues after stained. Skin slices were stained with Hematoxylin (G1080, Solarbio, China) and Eosin (H&E) stain (G1110, Solarbio, China) and Masson's trichrome (Masson) stain (G1346, Solarbio, China). H&E staining observed the pathological changes. Masson staining detected the renal collagen fibers.

For immunohistochemistry, the slices were heat-induced epitope retrieval and incubated with primary antibody for wnt4 (1:200, 14371-1-AP, Proteintech, China) overnight at 4°C. Secondary antibody for goat anti-rabbit immunoglobulin G (1:200, Sungene Biotech, China) was used to incubate the tissues for 1 hour at 37°C. Subsequently, the immunoactivity was observed by Chromogen diamino-benzidine (DAB, ZLI-9019, ZSGB-BIO, Beijing, China) and hematoxylin was used for nuclear staining.

Immunofluorescence of skin tissue was incubated with primary antibodies CD31 (1:200, GB113151, Servicebio, China) and CD146 (1:200, ab75769, Abcam), then maintained with corresponding secondary antibodies, and DAPI (Solarbio, Beijing, China) was used for staining nucleus. Immunofluorescence of CD31 (a marker of endothelial cells) and CD146 (a marker of pericytes) were performed to evaluate angiogenesis and mature vessels during wound healing of rats. The optical microscope and fluorescence microscope (Olympus, Tokyo, Japan) were used to detect the sections, and Image-analysis software was used for images quantified.

Cell culture and groups. The human umbilical vein endothelial cell (HUVEC, BNCC342247) line and human cerebrovascular pericytes (HBVPs, BNCC357532) were purchased from the BeiNa Culture Collection (Beijing, China). The HBVPs were cultured in Dulbecco's Modified Eagle Media (DMEM, Gibco, USA) containing 5.5 mmol/L glucose, 10% exosome-free serum (C3801-0100, VivaCell, IL), 100 U/mL penicillin, and 100μg/mL streptomycin (C100C5, NCM Biotech, China). HUVEC cells were maintained in endothelial cell medium (ECM, 1001, SienceCell, USA) containing 5% exosome-free fetal bovine serum (FBS, 10091-148, Gibco, USA), and 1% endothelial cell growth supplement (ECGS) and 1% penicillin-streptomycin solution (C100C5, NCM Biotech, China). Cells were all cultured at a condition with 37°C, 5% CO_2 and 95% humidity.

The HBVPs were designed into normal glucose group served as the control (CON) group, high glucose (HG) group, high mannitol (HM) group, AD group and HG+AD group, and HBVPs all maintained with exosome-free FBS. Cells in CON group were maintained in DMEM containing 5.5 mmol/L glucose, 10% exosome-free FBS, 1% penicillin-streptomycin solution. Cells in HG group were maintained in DMEM containing 33.3 mmol/L glucose, 10% exosome-free FBS, and 1% penicillin-streptomycin solution. Cells in HM group were incubated with DMEM containing 5.5 mmol/L glucose and 27.8 mmol/L mannitol, 10% exosome-free FBS and 1% penicillin-streptomycin solution. Cells for AD group were cultured in 5.5 mmol/L glucose medium containing 200ug/ml AD. The HG+AD group was cultured in DMEM containing 33.3 mmol/L glucose with 200ug/ml AD. The 33.3 mmol/L glucose concentrations and

concentrations of AD (200 ug/ml) we used according to the Cell Counting Kit 8 (CCK8) assay **(Figure4A, 4B)**.

Exosome Extraction and Identification. Exosome extraction kit (TransExo^{TM} Cell Media Exosome Kit, FE401, TransGen Biotech, China) was utilised to extract exosomes from HBVPs 48 hours after interventions. The supernatant of P3-P7 HBVPs was collected, and a 2:1 ratio of exosome precipitation solution-cell media was added overnight (>12 hours) at 4°C. To remove all liquid, the mixture was centrifuged at 10000g for 30 minutes at 4°C. The exosome mixture was subsequently resuspended by adding precipitation to 100-500 L PBS to resuspend the exosomes. Finally, exosome resuspension solution-cell media was added to the exosome mixture in order to obtain HBVPs exosome (HBVPs-exos). Using a BCA Protein Assay Kit (ZJ102L, EpiZyme, China), the concentrations of exosome suspension were determined. HBVPs-exos were utilised in further experiments or stored at -80°C. To determine the morphology, size distribution of exosomes, and exosomal markers (TSG101, ALIX, HSC70 and Calnexin), transmission electron microscopy (Hitachi, Japan), Nanoparticle tracking analysis (NTA), and Western blotting were used.

Exosome labeling and uptake. The exosomes extracted from HBVPs were labeled with the red membrane-labeling dye PKH26 (UR52302, Umibio, China). Subsequently, Diluent C containing the exosomes was mixed with PKH26 linker (PKH26 linker: Diluent C = 1:9) for 10 min at room temperature. The labeled exosomes of HBVPs were

added to exosome-free ECM medium. Finally, the above labeled exosomes ECM medium was added to HUVECs for 24h, which already seeded on a 6-wells plate and treated with various interventions. We maintained the cells with 4% paraformaldehyde, washed with PBS, and fixed with DAPI (C0065, Solarbio, China). Lastly, the ability of HUVECs to uptake exosomes derived from HBVPs was measured by the fluorescence microscope.

Cell viability in response to exosomes. The cell viability of the HUVECs in response to exosomes derived from HBVPs was measured by the CCK8 (C6005, NCM Biotech, China). Briefly, 3000 HUVECs were seeded in 96-wells plate and incubated with different concentrations of exosomes (0 μg/ml, 5 μg/ml, 10 μg/ml, 20 μg/ml, 30 μg/ml, and 40 μg/ml) extracted from HBVPs of various interventions in ECM medium for 24 h. Subsequently, 110 μl ECM medium containing 10 μl CCK-8 work solution was added and maintained at 37°C for 3 h. Finally, the microplate reader (Bio-Rad, USA) was used to detect the wavelength at 450 nm.

Wound Healing Assay. When the HUVECs reached 100% confluence, a sterile 200 μl micropipette tip was used to create wounds in a six-well plate. The floating cells were washed with PBS, and a 6-well plate containing fresh ECM medium containing exosomes extracted from HBVPs was added. Based on the exosomes extracted from HBVPs, the HUVECs were classified into six groups:1) No-Exo group: without exosomes; 2) CON-Exo group: added exosomes extracted from HBVPs maintained in 5.5

mmol/L glucose; 3) HG-Exo group: added exosomes extracted from HBVPs maintained in 33.3 mmol/L glucose; 4) HM-Exo group: added exosomes extracted from HBVPs maintained in 5.5 mmol/L glucose and 27.8 mmol/L mannitol; 5) AD-Exo group: added exosomes extracted from HBVPs maintained in 5.5 mmol/L glucose medium containing 200ug/ml AD; and 6) HG+AD-Exo group: added exosomes extracted from HBVPs maintained in 33.3 mmol/L glucose medium containing 200ug/ml AD. An optical microscope (Olympus, Tokyo, Japan) was used to observe the wound area at 0 and 24 hours. Lastly, the ImageJ software was utilized to assess the wound closure.

Tube formation assay. In vitro neovascularization assays of HUVECs were measured by Matrigel (354234, Corning, USA). Firstly, HUVECs incubated with exosomes extracted from HBVPs for 48 h. After intervention, HUVECs were seeded into 48-wells plate coated with Matrigel for 6 h. Lastly, the inverted microscope (Olympus, Tokyo, Japan) was used to observe the capillary-like structure formation and ImageJ Software was conducted to quantify the number of nodes and length of tubes.

Inhibition of Wnt/β-catenin signaling pathway in vitro. The inhibitor of Wnt/β-catenin signaling pathway (XAV939, Sigma, USA) was used to verify the effects of AD in wound healing. The HUVECs were cultured in 6-wells plate with ECM medium containing different interventions at 37°C in a humidification atmosphere containing 5% CO_2 for 48 h. Western blotting was used to measure the signaling pathway.

Western Blot Analysis. Total proteins from HUVECs and skin tissues were extracted by RIPA lysis buffer containing phosphatase inhibitors, PMSF and loading buffer. Proteins were loaded equally into the 10% SDS polyacrylamide gels, and transferred onto nitrocellulose membranes. After blocking with 5% skimmed milk in 0.1% tris buffered saline tween for 1 h, subsequently, the membranes were incubated at 4°C overnight with primary antibodies, including: TSG101 (1:1000, ab125011, Abcam), ALIX (1:1000, ab275377, Abcam), HSC70 (1:1000, ab51052, Abcam), Calnexin (1:1000, ab133615, Abcam), Wnt4 (1:2000, A7809, ABclonal, China), β-catenin (1:1000, M24002, Abmart, China), cyclin D1 (1:1000, A19038, ABclonal, China), and β-actin (1:1000, 8H10D10, Cell Signaling). After washing, the membranes were incubated for 1 h with the normal isotype-matched biotinylated secondary antibodies (both 1:4000, Sungene Biotech, China). Finally, the chemiluminescence reagent (Advansta, CA, USA) was used to observe the immunoblots and ImageJ software was utilized to quantify blots.

Statistical Analysis. GraphPad Prism 8.0.1 software (GraphPad, San Diego, CA, USA) were conducted to analyze all data. Data are shown as the mean ± standard deviation (x ± SD). One-way ANOVA analysis was used to evaluate the significance of the results. $P < 0.05$ was defined as statistically significance.

Data availability

The datasets used and/or analysed during the current study available from the corresponding author on reasonable request.

References

1. Qiu, J., Shu, C., Li, X., Ye, C. & Zhang, W. C. Exosomes from linc00511-overexpressing ADSCs accelerates angiogenesis in diabetic foot ulcers healing by suppressing PAQR3-induced Twist1 degradation. *Diabetes Res Clin Pract* **180**, 109032, http://doi.org/10.1016/j.diabres.2021.109032 (2021).
2. Lotfy, M., Adeghate, J., Kalasz, H., Singh, J. & Adeghate, E. Chronic Complications of Diabetes Mellitus: A Mini Review. *Curr Diabetes Rev* **13**, 3-10, http://doi.org/10.2174/1573399812666151016101622 (2017).
3. Bardill, J. R. *et al.* Topical gel-based biomaterials for the treatment of diabetic foot ulcers. *Acta Biomater* **138**, 73-91, http://doi.org/10.1016/j.actbio.2021.10.045 (2022).
4. Yang, J. Y., Chen, Z. Y., Pan, D. Y., Li, H. Z. & Shen, J. Umbilical Cord-Derived Mesenchymal Stem Cell-Derived Exosomes Combined Pluronic F127 Hydrogel Promote Chronic Diabetic Wound Healing and Complete Skin Regeneration. *Int J Nanomed* **15**, 5911-5926, http://doi.org/10.2147/Ijn.S249129 (2020).
5. Frykberg, R. G. *et al.* Diabetic foot disorders. A clinical practice guideline (2006 revision). *J Foot Ankle Surg* **45**, S1-66, http://doi.org/10.1016/S1067-2516(07)60001-5 (2006).
6. Davis, F. M., Kimball, A., Boniakowski, A. & Gallagher, K. Dysfunctional Wound Healing in Diabetic Foot Ulcers: New Crossroads. *Current Diabetes Reports* **18**, http://doi.org/10.1007/s11892-018-0970-z (2018).
7. Boulton, A. J. M., Vileikyte, L., Ragnarson-Tennvall, G. & Apelqvist, J. The global burden of diabetic foot disease. *Lancet* **366**, 1719-1724, http://doi.org/10.1016/s0140-6736(05)67698-2 (2005).
8. Liu, Z. J. & Velazquez, O. C. Hyperoxia, endothelial progenitor cell mobilization, and diabetic wound healing. *Antioxid Redox Sign* **10**, 1869-1882, http://doi.org/10.1089/ars.2008.2121 (2008).
9. Okonkwo, U. A. & DiPietro, L. A. Diabetes and Wound Angiogenesis. *International Journal of Molecular Sciences* **18**, http://doi.org/ARTN

141910.3390/ijms18071419 (2017).

10. Castilla, D. M., Liu, Z. J. & Velazquez, O. C. Oxygen: Implications for Wound Healing. *Adv Wound Care (New Rochelle)* **1**, 225-230, http://doi.org/10.1089/wound.2011.0319 (2012).
11. Mayo, J. N. & Bearden, S. E. Driving the Hypoxia-Inducible Pathway in Human Pericytes Promotes Vascular Density in an Exosome-Dependent Manner. *Microcirculation* **22**, 711-723, http://doi.org/10.1111/micc.12227 (2015).
12. Li, D. Y. & Wu, N. Mechanism and application of exosomes in the wound healing process in diabetes mellitus. *Diabetes Res Clin Pr* **187**, http://doi.org/ARTN 10988210.1016/j.diabres.2022.109882 (2022).
13. Trost, A., Bruckner, D., Rivera, F. J. & Reitsamer, H. A. Pericytes in the Retina. *Adv Exp Med Biol* **1122**, 1-26, http://doi.org/10.1007/978-3-030-11093-2_1 (2019).
14. Huang, H. Pericyte-Endothelial Interactions in the Retinal Microvasculature. *Int J Mol Sci* **21**, http://doi.org/10.3390/ijms21197413 (2020).
15. Ye, L. *et al.* Exosomal circEhmt1 Released from Hypoxia-Pretreated Pericytes Regulates High Glucose-Induced Microvascular Dysfunction via the NFIA/NLRP3 Pathway. *Oxidative Medicine and Cellular Longevity* **2021**, http://doi.org/Artn 883309810.1155/2021/8833098 (2021).
16. Jere, S. W. & Houreld, N. N. Regulatory Processes of the Canonical Wnt/beta-Catenin Pathway and Photobiomodulation in Diabetic Wound Repair. *International Journal of Molecular Sciences* **23**, http://doi.org/ARTN 421010.3390/ijms23084210 (2022).
17. Igota, S. *et al.* Identification and Characterization of Wnt Signaling Pathway in Keloid Pathogenesis. *Int J Med Sci* **10**, 344-354, http://doi.org/10.7150/ijms.5349 (2013).
18. Zhang, H. *et al.* Regulatory Mechanisms of the Wnt/beta-Catenin Pathway in Diabetic Cutaneous Ulcers. *Frontiers in Pharmacology* **9**, http://doi.org/ARTN 111410.3389/fphar.2018.01114 (2018).
19. Chong, Z. Z., Shang, Y. C. & Maiese, K. Vascular injury during elevated glucose can be mitigated by erythropoietin and Wnt signaling. *Curr Neurovasc Res* **4**, 194-

204 (2007).

20. Yang, S. *et al.* Insulin Promotes Corneal Nerve Repair and Wound Healing in Type 1 Diabetic Mice by Enhancing Wnt/beta-Catenin Signaling. *Am J Pathol* **190**, 2237-2250, http://doi.org/10.1016/j.ajpath.2020.08.006 (2020).
21. Zhang, B. *et al.* Human Umbilical Cord Mesenchymal Stem Cell Exosomes Enhance Angiogenesis Through the Wnt4/beta-Catenin Pathway. *Stem Cell Transl Med* **4**, 513-522, http://doi.org/10.5966/sctm.2014-0267 (2015).
22. Zhao, A. H., Zhang, Y. B. & Yang, X. W. Simultaneous determination and pharmacokinetics of sixteen Angelicae dahurica coumarins in vivo by LC-ESI-MS/MS following oral delivery in rats. *Phytomedicine* **23**, 1029-1036, http://doi.org/10.1016/j.phymed.2016.06.015 (2016).
23. Hou, M. *et al.* Pharmacodynamic action and mechanism of Du Liang soft capsule, a traditional Chinese medicine capsule, on treating nitroglycerin-induced migraine. *J Ethnopharmacol* **195**, 231-237, http://doi.org/10.1016/j.jep.2016.11.025 (2017).
24. Lee, B. W. *et al.* Antiviral activity of furanocoumarins isolated from Angelica dahurica against influenza a viruses H1N1 and H9N2. *J Ethnopharmacol* **259**, http://doi.org/ARTN 11294510.1016/j.jep.2020.112945 (2020).
25. Zhang, X. N. *et al.* Angelica Dahurica ethanolic extract improves impaired wound healing by activating angiogenesis in diabetes. *Plos One* **12**, http://doi.org/ARTN e017786210.1371/journal.pone.0177862 (2017).
26. Guo, J. *et al.* Angelica dahurica promoted angiogenesis and accelerated wound healing in db/db mice via the HIF-1 alpha/PDGF-beta signaling pathway. *Free Radical Bio Med* **160**, 447-457, http://doi.org/10.1016/j.freeradbiomed.2020.08.015 (2020).
27. Thomas, H. M., Cowin, A. J. & Mills, S. J. The Importance of Pericytes in Healing: Wounds and other Pathologies. *International Journal of Molecular Sciences* **18**, http://doi.org/ARTN 112910.3390/ijms18061129 (2017).
28. Braverman, I. M., Sibley, J. & Keh, A. Ultrastructural analysis of the endothelial-pericyte relationship in diabetic cutaneous vessels. *J Invest Dermatol* **95**, 147-153, http://doi.org/10.1111/1523-1747.ep12477903 (1990).

29. Wei, P. *et al.* Exosomes derived from human amniotic epithelial cells accelerate diabetic wound healing via PI3K-AKT-mTOR-mediated promotion in angiogenesis and fibroblast function. *Burns Trauma* **8**, http://doi.org/ARTN tkaa02010.1093/burnst/tkaa020 (2020).

30. Hu, Y. Q. *et al.* Exosomes derived from pioglitazone-pretreated MSCs accelerate diabetic wound healing through enhancing angiogenesis. *J Nanobiotechnol* **19**, http://doi.org/ARTN 15010.1186/s12951-021-00894-5 (2021).

31. Bo, Y. Y. *et al.* Exosomes from human induced pluripotent stem cells-derived keratinocytes accelerate burn wound healing through miR-762 mediated promotion of keratinocytes and endothelial cells migration. *J Nanobiotechnol* **20**, http://doi.org/ARTN 29110.1186/s12951-022-01504-8 (2022).

32. Li, Q. J. *et al.* Exosome loaded genipin crosslinked hydrogel facilitates full thickness cutaneous wound healing in rat animal model. *Drug Deliv* **28**, 884-893, http://doi.org/10.1080/10717544.2021.1912210 (2021).

33. Chao, Y. H., Yang, W. T., Li, M. C., Yang, F. L. & Lee, R. P. Angelica dahurica and Rheum officinale Facilitated Diabetic Wound Healing by Elevating Vascular Endothelial Growth Factor. *Am J Chinese Med* **49**, 1515-1533, http://doi.org/10.1142/S0192415x21500713 (2021).

34. Yang, W. T., Ke, C. Y., Wu, W. T., Tseng, Y. H. & Lee, R. P. Antimicrobial and anti-inflammatory potential of Angelica dahurica and Rheum officinale extract accelerates wound healing in Staphylococcus aureus-infected wounds. *Sci Rep-Uk* **10**, http://doi.org/ARTN 559610.1038/s41598-020-62581-z (2020).

35. Wu, M. F. *et al.* Ruyi Jinhuang Powder accelerated diabetic ulcer wound healing by regulating Wnt/beta-catenin signaling pathway of fibroblasts In Vivo and In Vitro. *J Ethnopharmacol* **293**, http://doi.org/ARTN 11532110.1016/j.jep.2022.115321 (2022).

36. Yang, P., Li, S. Y., Zhang, H., Ding, X. F. & Tan, Q. LRG1 Accelerates Wound Healing in Diabetic Rats by Promoting Angiogenesis via the Wnt/beta-Catenin Signaling Pathway. *Int J Low Extr Wound*, http://doi.org/Artn 153473462210816101010.1177/15347346221081610 (2022).

37. Zhang, B. *et al.* HucMSC-Exosome Mediated-Wnt4 Signaling Is Required for Cutaneous Wound Healing. *Stem Cells* **33**, 2158-2168, http://doi.org/10.1002/stem.1771 (2015).
38. Kretzschmar, K. & Clevers, H. Wnt/beta-catenin signaling in adult mammalian epithelial stem cells. *Dev Biol* **428**, 273-282, http://doi.org/10.1016/j.ydbio.2017.05.015 (2017).
39. Cheon, S. S. *et al.* Beta-catenin regulates wound size and mediates the effect of TGF-beta in cutaneous healing. *Faseb J* **20**, 692-701, http://doi.org/10.1096/fj.05-4759com (2006).
40. Fathke, C. *et al.* Wnt signaling induces epithelial differentiation during cutaneous wound healing. *Bmc Cell Biol* **7**, http://doi.org/Artn 410.1186/1471-2121-7-4 (2006).
41. Genovese, P. *et al.* Co-delivery of fibrin-laminin hydrogel with mesenchymal stem cell spheroids supports skeletal muscle regeneration following trauma. *J Tissue Eng Regen M* **15**, 1131-1143, http://doi.org/10.1002/term.3243 (2021).

Acknowledgments

The authors thank all colleagues for their help in this study. We would like to thank the Tianjin Key Medical Discipline (Specialty) Construction Project for funding this work.

Author contributions

Congqing Pan contributed to designing the experiment, supervising the experimentators, and interpreting the results. Wangna Tang and Junfen Liu conducted the experiment, analyzed the data. Wangna Tang drafted the manuscript, Wangna Tang, Junfen Liu and Cailing Gao corrected the draft. Cailing Gao participated in the discussion of the results and revision of the manuscript. Wenjie Liu and Linlin Wang assisted in analyzing the data. All data were generated in-house, and no paper mill was used. All

authors agree to be accountable for all aspects of work ensuring integrity and accuracy.

Funding

This work was supported by the National Natural Science Foundation of China (No. 81873304) and Zhangjiakou City Key R&D Program Project (No.2121074D).

Competing interests

The authors report no conflicts of interest in this work.

Figure legends

Figure 1: AD promotes wound healing and structural improvement in STZ rats. **(A)** Representative images showing the healing process with AD-treated rats on different days. **(B)** Representative analysis of the wound healing rates. **(C)** Representative images (100×) of HE staining of skin tissues. The scale bar shows 50 μm. **(D)** Representative images (100×) of Masson staining of skin tissues. The scale bar shows 50 μm. *$p < 0.05$ vs. CON group; $^{\#}p < 0.05$ vs. STZ group. Data are expressed as mean ± SD (n = 10).

Figure 2: AD increases the angiogenesis in STZ rats. **(A, B)** Representative images (100×) showing immunohistochemistry of Wnt4 in skin tissues (scale bar = 50 μm). **(C)** Immunofluorescence images (100×) of β-catenin (red) in skin tissues. The scale bar shows 50μm. **(D, E)** Immunohistochemical images (100×) of CD31 (red) and CD146 (green) in the wound vessels (scale bar = 50 μm). *$p < 0.05$ vs. CON group; $^{\#}p < 0.05$

vs. STZ group. Data are expressed as mean ± SD (n = 10).

Figure 3: AD boosts angiogenesis through Wnt4/β-catenin pathway in vivo. **(A)** Western blot analysis of Wnt4, β-catenin, and cyclinD1 protein levels in the wound skin tissues. **(B)** Quantitation of protein levels in **(A)**. *$p < 0.05$ vs. CON group; $^{\#}p < 0.05$ vs. STZ group. Data are expressed as mean ± SD (n = 10).

Figure 4: The characterization of exosome derived from HBVPs. **(A, B)** The viability of HBVPs separately maintained with different concentrations of glucose (A) and AD maintained in 33.3 mmol/L glucose medium (B) for 48 h. *$p < 0.05$ vs. 5.5 mmol/L group, $^{\#}P<0.05$ vs the 33.3 mmol/L group. **(C)** Western blot of HBVPs-derived exosome markers. **(D)** The amount of exosome secretion quantified by BCA protein quantity. **(E)** Representative electron microscopy images of exosomes derived from HBVPs (scale bar = 200 nm). **(F)** The size distribution of exosomes determined by Nanoparticle tracking analysis.

Figure 5: Exosome ingestion and the effects of exosome derived from HBVPs on HUVECs vitality. **(A)** Fluorescence images (100X) of exosome ingested by HUVECs. Blue, nuclei. Red, exosomes. **(B)** Cell viability of the HUVECs in response to exosomes derived from HBVPs. *$p < 0.05$ vs. 0 μg/ml group.

Figure 6: AD promotes the migration and angiogenic tubule formation of HUVECs by regulating exosomes derived from HBVPs. **(A, C)** Wound healing assay is used to detect cell migration under exosomes derived from HBVPs. **(B, D)** Migration rate (%) of cell migration by wound healing assay. *$P<0.05$ vs the CON Exo group, $^{\#}P<0.05$ vs the HG Exo group. **(E, H)** Representative images of tube formation under exosomes

derived from HBVPs. **(F, G)** Quantitation of the number of nodes and the length of tubes. *P<0.05 vs the NO Exo group, $^{\#}P$<0.05 vs the CON Exo group. **(I, J)** Quantitation of the number of nodes and the length of tubes. *P<0.05 vs the CON Exo group, $^{\#}P$<0.05 vs the HG Exo group.

Figure 7: AD improves the angiogenesis by regulating pericyte-endotheliocyte exosomes crosstalk through Wnt4/β-catenin signal pathway. **(A)** Western blot analysis of Wnt4, β-catenin, and cyclinD1 protein levels in the HUVECs. **(B-D)** Quantitation of protein levels in **(A)**. *P<0.05 vs the CON Exo group, $^{\#}P$<0.05 vs the HG Exo group, $^{\&}P$<0.05 vs the AD Exo group. **(E)** Representative Wnt4, β-catenin, and cyclinD1 protein expression by Western blot in HUVECs following XAV939 inhibition. **(F-H)** Quantitation of protein levels in (C). *P<0.05 vs the CON Exo group, $^{\#}P$<0.05 vs the HG Exo group, $^{\&}P$<0.05 vs the HG+AD Exo group.

FigureS1: The levels of blood parameters in STZ rats after wound. Note: S 0d: the day before STZ intraperitoneal injection; S 7d: the 7^{th} day after STZ intraperitoneal injection; S 18d: the 18^{th} day after STZ intraperitoneal injection; W 0d: the day before the wound; W 11d: the 11^{th} day after the wound. *P<0.05 vs the CON group.

Gels and blots have been cut. Original blots are presented in Supplementary File.

Supplementary Files

This is a list of supplementary files associated with this preprint. Click to download.

- FigureS1.pdf